Improved Reservoir Characterization from Integration of Towed Streamer EM and Dual-sensor Broadband Seismic Data

Z. Du* (PGS), G. Namo (Former PGS), V. Charoing (PGS), C. Reiser (PGS)

Summary

We present a data integration study for reservoir characterization, resulting in estimates of hydrocarbon saturation in place within a reservoir. The limitations of using only seismic data for detailed reservoir characterization are well recognized. Seismic data are well suited to resolving structure and some rock properties, notably porosity, but attempts to map fluids from seismic data may be misleading due to the ambiguity between fluid and lithology effects. It is well known that CSEM data are sensitive to the presence of hydrocarbons, but the diffusive energy propagation results in low resolution images. Thus, a careful combination of both types of data helps to overcome their individual weaknesses. In this paper, we outline with a dataset example how the CSEM and seismic data can be integrated together with limited rock physical knowledge in the prospect area to estimate the total volume of hydrocarbon in place.

Introduction

An understanding of reservoir characteristics, most importantly, porosity, water saturation, and thickness and lateral extension of the reservoir are crucial factors in reservoir characterization. These parameters are important because they serve as veritable inputs for reservoir volumetric analysis, i.e. the volume of hydrocarbon in place. The limitations of using seismic data for detailed reservoir characterization are well recognized. Seismic data are well suited to resolving structure and some rock properties, notably porosity, but attempts to map fluids from seismic data may be misleading due to the ambiguity between fluid and lithology effects. It is well known that CSEM data are sensitive to the presence of hydrocarbons, but the diffusive energy propagation results in low resolution images. A careful combination of both types of data helps to overcome their individual weaknesses.

The discovery of the Skrugard accumulation (which now together with the Havis discovery is called Johan Castberg) was a major milestone in the exploration of the Barents Sea. The Johan Castberg area is located in the PL532 license as shown in Figure 1a. The Skrugard discovery is located within the Bjørnøyrenna Fault Complex on the crest of a north–south-trending rotated fault block partly eroded. A combination of structural tilting of the Realgrunnen Subgroup reservoirs containing the Stø, Nordmela and Tubåen formations, and truncation of the intra-Cretaceous unconformities at the crest of the fault block, has formed the Skrugard trap. The structural apex is at 1,204 mMSL, and the elongated four-way closure covers an area of ~14 km^2. The water depth in the area is ~370 m. The appraisal well 7220/5-1 was drilled in 2012 and encountered both gas and oil. The reservoir zone interval containing hydrocarbons was ~100 m thick in most of the structure.

Field data

Over the years, PGS has started to build- up a substantial Towed Streamer EM multi-client library in the Barents Sea. As part of a larger acquisition campaign in 2013, nearly 850-line km of Towed Streamer EM and broadband dual-sensor towed streamer seismic data were acquired simultaneously using a single vessel over a number of known discoveries, including Skrugard (Figure 1a). The Towed Streamer EM system consists of an 800 m long horizontal electric dipole (HED) towed at 10 m and an EM streamer towed at 100 m water depth, both of which are towed from a single vessel. The streamer has 72 electric field channels, or electrode pairs, providing offsets from ~500-7708 m relative to the centre of the source. The source transmits an optimized repeated sequence (ORS) generated by an oscillating current of +/- 1500 A at a frequency range of two decades (0.1-10 Hz). Having a shot cycle of 120 seconds and an acquisition speed of 4-5 knots the average shot distance is ~250 m.

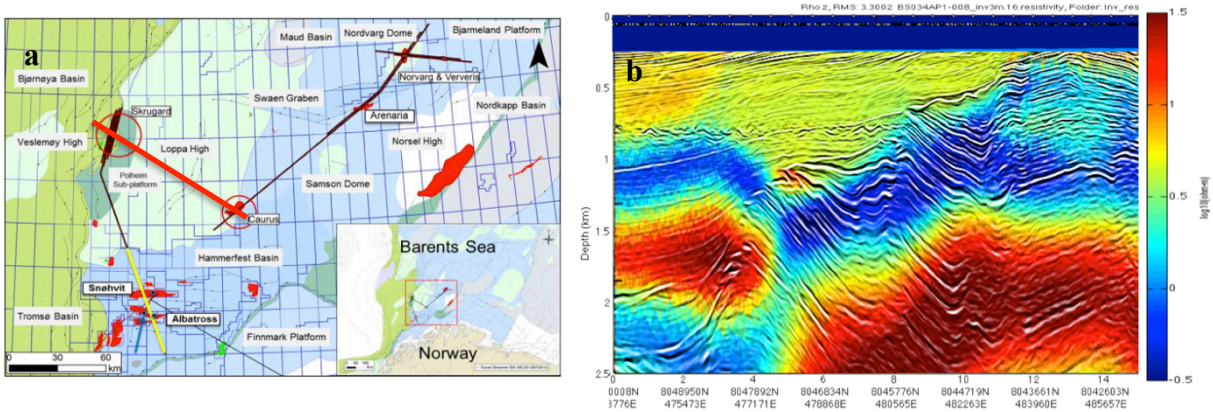

Figure 1. *(a) Map showing the Towed Streamer EM survey over Skrugard area in Barents Sea. (b) Vertical resistivity overlain on co-incident depth converted full-stack dual-sensor seismic data from seismic guided inversion for the survey line BS034 (thick red line in a) traversing Skrugard discovery.*

Towed Streamer EM data

Du and Hosseinzadeh (2014) described a Towed Streamer EM data inversion workflow designed to

make inversion-based EM process more data and information-driven and less a-priori model-driven. For the Skrugard area Towed Streamer EM data inversion, we applied a staged inversion workflow of increasing sophistication. First, we used an unconstrained inversion to obtain a resistivity section with depth. The unconstrained inversion does not take into account complex or higher dimensional structures, but allows the class of structures to which the data are most sensitive to be assessed. Secondly a seismic guided inversion was performed driven purely by the seismic and the EM data (Du and Hosseinzadeh, 2014; Mckay et al. 2015). The higher resolution of the seismic image makes it possible to suggest the most appropriate locations of potential resistivity contrasts, whereas a conventional constrained inversion adopts *a priori* model created by seismic to prejudice the EM inversion's roughness penalty to force resistivity variations to follow the major acoustic boundaries. In seismic guided inversion the resistivity variations within the seismically defined stratigraphic regions/layers are guided by plausible lower and upper resistivity boundaries suggested by unconstrained EM inversions. In this way, it maximizes the inversion-searching domain to ensure the use of the seismic only as a structural 'guider'. Figure 1b shows the vertical resistivity for the line BS034 (the thick red line in Figure 1a) determined using 2.5D inversion (for brevity horizontal resistivity is not shown) superimposed on the coincident full-stack seismic depth section. A prominent resistivity anomaly is recovered at the depth and laterally confined within the main reservoir fault block of the Skrugard.

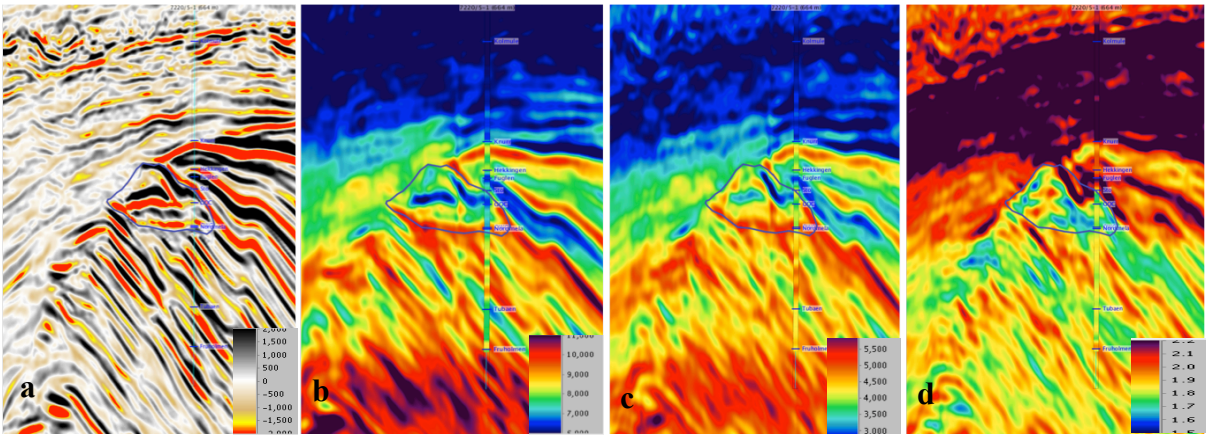

Figure 2. *Left to right: Near angle (a), P- wave impedance (Ip) (b), S- wave impedance (Is) (c) and Vp/Vs (d); and with the corresponding 7220/5-1 logs (thin line) superimposed. The black polygon identify reservoir container. In the P- wave impedance, the intra-reservoir shales appear yellow - red while the gas/oil sands are blue – green.*

Dual-sensor towed streamer seismic data

The seismic data shown in Figure 2 resulted from the survey line BS034 (the thick red line in Figure 1a), obtained by simultaneous data acquisition of EM and seismic. The seismic dataset is of good higher signal-to-noise (S/N) ratio. Four angle stacks were generated by stacking over the range of incident angles 5-15°, 15-25°, 25-35° and 35-45°, and inverted. In order to gain insight into the reservoir properties (e.g. porosity), inversion for both acoustic and shear (P and S) impedances is required and a low frequency information is also required for the computation of absolute elastic properties. A smooth background model was thus constructed by kriging the well 7220/5-1 data with the seismic along the interpreted horizons. The dual-sensor towed streamer seismic data has a seismic frequency bandwidth between 3 to 125 Hz, allowing a very small amount of low frequency information to obtain the absolute properties as the frequency gap is only between 0 and 3 Hz. Pre-stack seismic inversion simultaneously inverted for P- and S-impedance and the Vp/Vs ratio. As shown in Figure 2, both P and S impedances delimit very well the reservoir and flat spot, and the thicker intra-reservoir shales are well defined in the P wave impedance. This example demonstrates the advantages of using broadband acquired pre-stack data in deriving reliable pre-stack AVO inversion products for reliably retrieving the reservoir elastic properties.

Rock physics

The key for a successful integrated approach is a consistent rock physics framework. Geophysical properties of rocks, such as resistivity or elastic moduli, depend on mineralogy, pore fluid properties, and the geometry or fabric of the rock. Rock physics models are the transforms used to convert the rock and fluid description into geophysical properties.

Using data from the 7220/5-1 well, we constructed and validated acoustic and electric rock physics models for the Skrugard discovery. We varied fluids and lithology (particularly shale content) to investigate the sensitivity of the surface data to these quantities. These modelling processes helped to clarify where ambiguities are resolved by combining elastic and electrical data and where they remain unresolved, thus permitting assessment of the uncertainties in our final results.

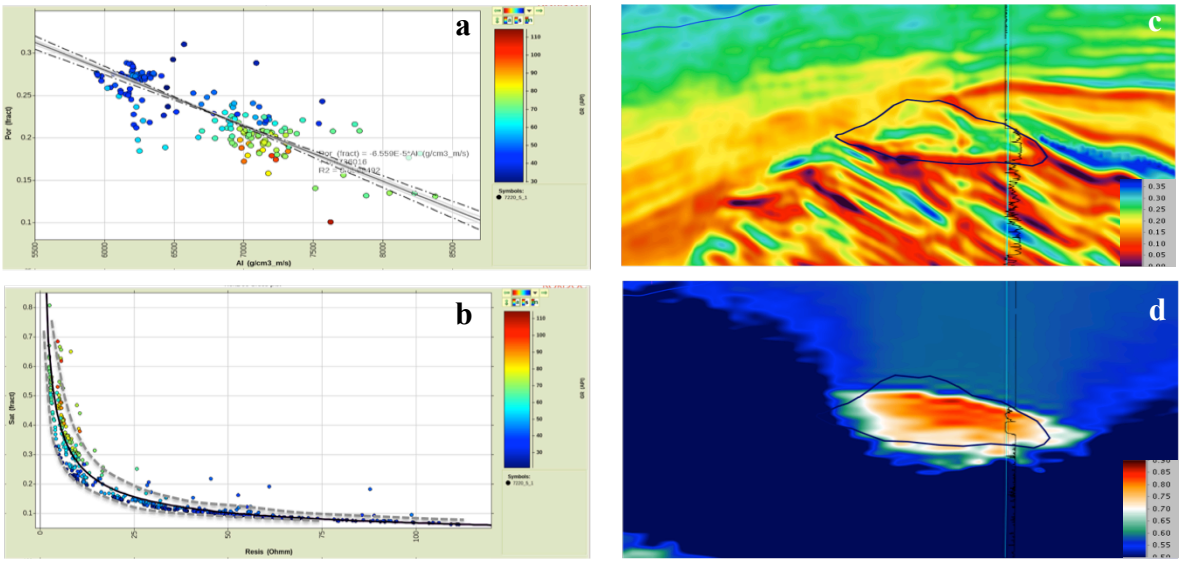

Figure 3. *Left, crossplot of porosity versus P-wave impedance for the reservoir interval with the dashed lines defining the 95% regression confidence interval (a); Water saturation versus resistivity with upper and lower bounds on saturation determined from the point cloud (b). Right: Porosity estimation from P-wave impedance with log overlay (c); hydrocarbon saturation estimation from the inverted vertical resistivity, water saturation log superimposed (d).*

In the case of the Skrugard discovery, the results of the EM and seismic inversions are combined through the rock physics models. The main shale units are identified in a cross-plot of P wave impedance versus Vp/Vs and thereafter excluded from the calibration. In the well, the linear correlation between P wave impedance and porosity is quite high, showing a correlation of 0.85 (Figure 3a). Upscaling well data with a running Backus average of velocities and density over a 10 m interval, and using an arithmetic running average of porosity only produces a small change in the linear relationship. Thus we feel comfortable to use the direct linear transform. Whereas we take into account the derivations (most likely the influence of the presence of clay within reservoir sands) from the determined mean by defining the 95% of the regression confidence interval as the lower and upper variation bonds of impedance-porosity plot (Figure 3a). Also, as we can observe, the relationship between resistivity and water saturation is complicated by the presence of the non-resolvable shales. This contributes to the uncertainty in hydrocarbon saturation estimates from the inverted EM resistivity. We therefore produce an upper and lower bounds on the resistivity-saturation plot from the inverted EM data, based on the cross-plot (Figure 3b). As these data include the shale influence, the bounds are considered reliable.

Data Integration

The results of applying the rock physics model and transform to the estimated reservoir rock fluid

property estimates away from well are shown in Figure 3c & d. The porosity is obtained from the acoustic impedance, whereas the hydrocarbon saturation is obtained from the resistivity. Notice the excellent matches to the well log-derived rock properties demonstrating that both porosity and saturation were correctly predicted. Figure 4a shows the hydrocarbon volume (HCV) display, i.e., the product of the porosity times saturation (Harries, et al. 2009). Figure 4b correspondingly describes the uncertainties of the estimation of the HCV using the lower and upper bounds of the resistivity-saturation and impedance-porosity transforms (Figure 3a & b). Due to lateral variation of the reservoir property, the uncertainties of the HCV become bigger away from the well location, as expected. The HCV mapped clearly the structures of the gas/oil spatial distribution. It shows that the accumulation of high hydrocarbon follows the complex Skrugard structural faulting (titled faults blocks) (see Figure 2a). We are here able through the data integration to recover the information on the presence of gas/oil within the reservoir at the seismic resolution.

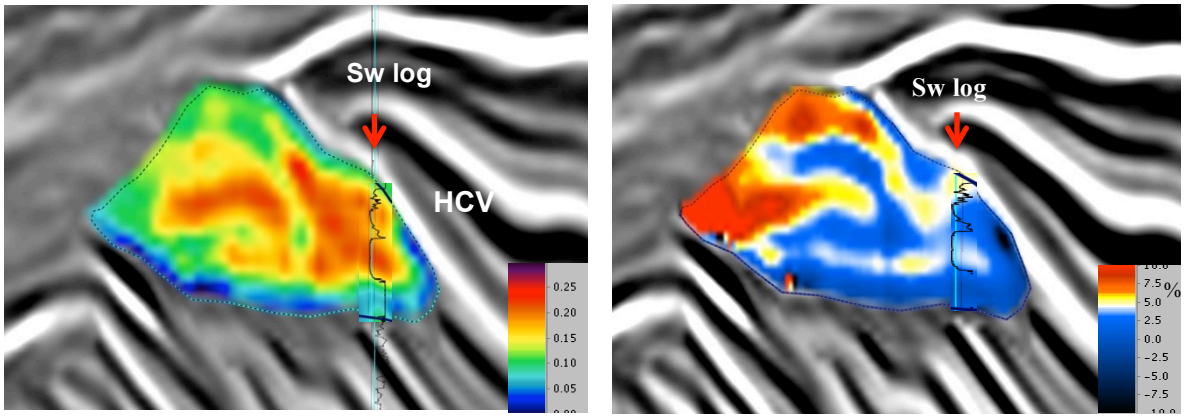

Figure 4. (a) *The hydrocarbon volume section derived from the data integration of CSEM and seismic inversions with the Sw log (well 7220/5-1) overlaid for comparison. The low saturation shales stand out clearly as the darker green events within the reservoir unit. (b) The uncertainties of HCV estimation from the rock physics integration (refer text for detail).*

Summary

There are currently increased high demanding that reservoir characterization and quantitative interpretation to go beyond simple images of structure, impedance and resistivity. Quantitative estimates of lithology and fluid properties are required in order to fully understand the character of a reservoir. In this abstract, we have presented an approach to integrate well log, seismic and CSEM data that permits estimates beyond those obtainable from just one type of data. The final product of this integrated workflow offers an estimate of total volume of hydrocarbon in place within a reservoir.

Acknowledgement
The author would like to thank PGS for allowing the publication of this paper, and thank for Bluegreen Geophysics for the MARE2DEM codes. Integrated products and services provided under license from Rock Solid Images Inc, to patent numbers US8064287, US7912649 and US12/135,729 and their related families.

References

Du, Z and Hosseinzadeh, S. [2014] Seismic guided EM inversion in complex geology: Application to the Bressay and Bentley heavy oil discoveries, North Sea, *75th EAGE Conference*, Expanded Abstract.

Harris,P., Du, Z., MacGregor, L., Olsen, Shu, R. and Cooper, R. [2009] Joint interpretation of seismic and CSEM data using well log constraints: an example from the Luva Field, *First Break*, 27, 73-81.

Mckay, A., Mattsson, J. and Du, Z. [2015] Towed Streamer EM – reliable recovery of sub-surface resistivity, *First Break*, 33, 75-85.